Orographic Rainfall, Deep-seated Catastrophic Landslides, and Landscape Evolution: Geomorphic Hazard Assessment in Active Orogens

Yuki MATSUSHI,[1,2,*] Masahiro CHIGIRA[1] and Ken'ichirou KOSUGI[2,3]

[1] Disaster Prevention Research Institute, Kyoto University (Gokasho, Uji, Kyoto 6110011, Japan.)

[2] CREST, JST (K's Gobancho, 7 Gobancho, Chiyoda-ku, Tokyo 1020076, Japan)

[3] Graduate School of Agriculture, Kyoto University (Kitashirakawa Oiwake-cho, Sakyo-ku, Kyoto 6068502, Japan)

*Corresponding author. E-mail: matsushi@slope.dpri.kyoto-u.ac.jp

The relationships between orographic rainfall, deep-seated landslides, and landscape evolution is examined in high-relief steep mountainous areas underlain by accretionary sedimentary rocks. Deep-seated landslides caused by an extreme rainfall in 2011 in Kii Mts shows a distribution that is distinctly different from the spatial pattern of orographic rainfall. The landslide distribution is better explained by rainfall anomaly defined as ratio to the maximum-class daily rainfall rather than absolute total rainfall amount. Landslides are prone to occur at outer rim around the enhanced rainfall center, exhibiting a pre-mature landscape with moderate relief and steepness, where hillslopes are characterized by inner-gorges formed by river incision. A similar slope form is common in a incised valley-side dip slopes along a major active fault in the western part of Hira Range. A simple stability modeling of wedge failure explains well the sliding or deformation of hillslopes, indicating the major control of slope-undercutting on bedrock landsliding. The most probable strength parameters are comparable to that of highly weathered rock mass, implying importance of geologic discontinuity with weak asperity in the bedrock for initiation of a deep-seated catastrophic landslide.

Key words: deep-seated catastrophic landslide, orographic rainfall, topographic relief, river incision, landscape evolution

1. INTRODUCTION

High-relief steep hillslopes in tectonically active areas are prone to cause deep-seated catastrophic landslides (i.e., bedrock sliding at a high speed with a long runout distance), especially where the terrains are underlain by accretionary sedimentary rocks and are deeply incised by river networks. Before rainfall or an earthquake triggers a landslide, the hillslopes deform gravitationally as a part of long-term geomorphic process [*Chigira*, 1992, 2000, 2009; *Chigira et al.*, 2013a]. Such gravitational slope deformation seems to progress through development of disintegrated and pulverized zones in the bedrock, forming an immature, intermittent shear plane sub-parallel to the slope surface [*Chigira et al.*, 2013b]. In many cases both of these potential slip plane and actual slip surface of deep-seated landslides appear on a line extending to the slope toe, at the bottom of the nearby incised valley. This observation implies that the slope deformation and subsequent landslides occur, being associated with long-term river incision [*Hiraishi and Chigira*, 2011].

Downslope displacement of unstable block on the developing slip plane results in exhibition of arched open-to-downward scarplets on the slope surface. The scarplets typically have an extent of dozens to hundreds of meters but less than few meters in slippage or subsidence of the moving body. Recent advance in air-borne laser scanning of ground surface provides a crucial advantage in searching such indiscernible topographic signals and thus may contribute to locate potential sites of deep-seated catastrophic landslides. Indeed several recent landslides caused by heavy rainfall were found to form their slip scarps at locations exactly coincide with the preceding deformation scaplets [*Chigira*, 2009; *Sasahara et al.*, 2012; *Chigira et al.*, 2013a].

Analyses of topography, slope form, and locations of landslide scars and/or deformation scarplets on hillslopes using GIS (Geographic

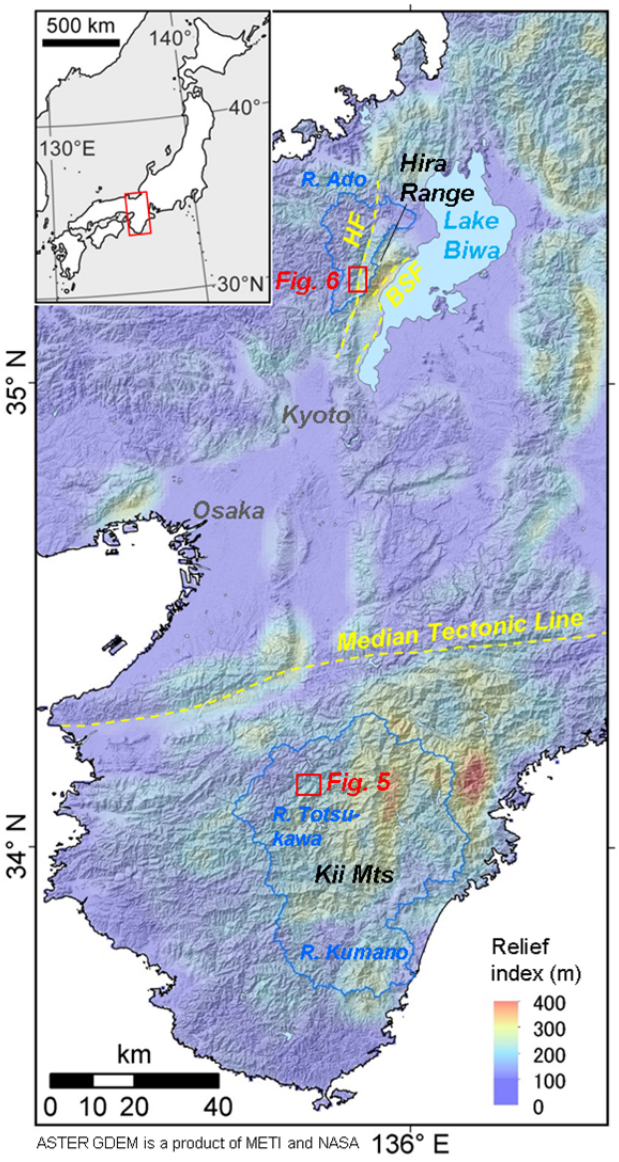

Fig. 1 Topographic relief map of the Kinki District, central Japan. The study areas are located in the mid Totsukawa River, Kii Mts, and western Hira Range. The relief index was calculated as standard deviation of altitude within a 100 km^2 circle window.

Information Systems) may provide a clue to understand causal relationships between river incision, development of relief and hillslope gradient, gravitational slope deformation, and deep-seated catastrophic landslides. Regional tectonics and rainfall system are most important factors for incision of fluvial channels and subsequent bedrock landslides, and thus control spatial pattern of topographic relief [*Burbank et al.*, 2003; *Gabet et al.*, 2004]. This implies existence of a feedback system between tectonics, climate, deep-seated landslides, and landscape evolution. Rainfall and earthquakes trigger landslides maintaining steep valley-side hillslopes. The resultant high rate of sediment yield and high-relief topography contribute to the enhancement of erosional isostatic uplift and orographic rainfall. These factors then affect river incision that destabilize the hillslopes in a long-term. This study aims to reveal how rainfall, landslides, and topography are linked, and discuss to what extent we can make hazard assessment in a geomorphological way. We focus on two typical mountainous terrains underlain by accretionary sedimentary rocks, subjected to high risk of deep-seated catastrophic landslides: central Kii Mountains and western Hira Range, as representative regions in outer and inner zones of SW Japan respectively.

2. STUDY AREA

The study areas are Kii Mountains and W-Hira Range, SW Japan [**Fig. 1**]. Bedrocks in both of these areas consist of accretionary sedimentary rocks, but are different in their age: Cretaceous to lower Miocene Shimanto Belt for Kii Mts, and Jurassic Tamba-Mino Belt for Hira Range. Topography in these area are dominated by high-relief (>200 m), steep (>30°) hillslopes. Rivers deeply incise the terrains to form gorges walled by steep lower side-slopes. This landscape is typical in both of the study areas especially in mid Totsukawa River in central Kii Mts, and in the western part of Hira Range, upper Adogawa River.

Both of these mountainous terrains are thought to have actively uplifted during the latest Cenozoic era. No active fault exists in the Kii Mts southerly from the Median Tectonic Line [**Fig. 1**]. However the Kii Mts seems to have upwarped as low relief gentle erosional surfaces are observed in higher elevations in the central part of the terrain. In the Hira Range, the mountainous terrain is bounded by two active strike-slip fault systems, Hanaore Fault (HF) to the west, Biwa-ko Seigan Fault (BSF) to the east [**Fig. 1**]. Because of the southward convergence of these fault systems, a extruded horst has uplifted to from the Hira Range with remaining low relief surfaces on its ridge crest.

In the Kii Mountains, Typhoon Talas hit the area from 31 Aug to 5 Sep 2011, and caused more than 70 deep-seated catastrophic landslides, by rainfall >2000 mm/4 days in maximum [**Fig. 2**]. Many of the landslides occurred during 3-4 Sep 2011, at the final stage of the rainfall event or timing within one day after the rainfall had stopped [*Yamada et al.*, 2012]. The volume of each landslide ranged from 10^5 upto 10^7 m^3 (with source areas from 1×10^4 to 4×10^5 m^2). A similar disaster occurred in 1889 with a

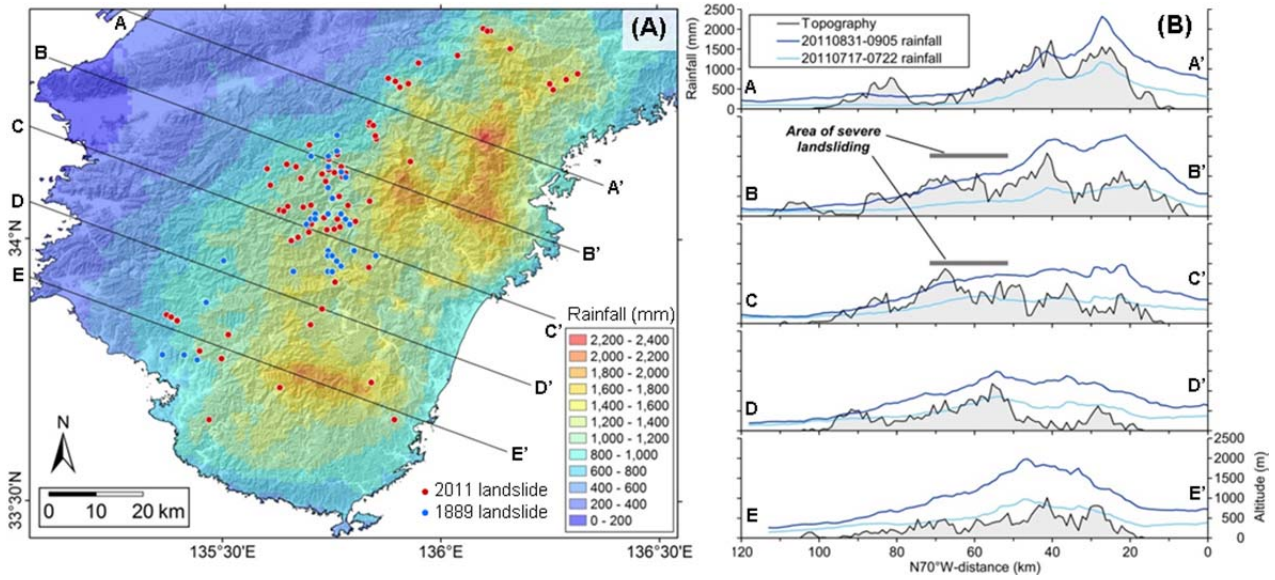

Fig. 2 Spatial distributions of orographic rainfall and deep-seated landslides in the Kii Mts. (A) Distribution of rainfall amount at the extreme-class rainfall event from 31 Aug to 5 Sep 2011, as typical spatial pattern of enhanced orographic rainfall in the Kii Mts. Red circles indicate locations of deep-seated catastrophic landslides at the 2011 event while blue circles are landslides at the 1889 event [*Tabata et al.,* 2002; *Mizuyama et al.,* 2011]. Landslides are located out around the orographic rainfall center. (B) Profiles of rainfall and topography. The orographic rainfall show similar spatial pattern but different only in the magnitude.

resembled distribution of landslides, caused by a typhoon with an almost identical reconstructed track to the 2011 event [*Hirano et al.*, 1984].

In the Hira Range, we have poor records of deep-seated catastrophic landslides. An earthquake in 1662 (Kanbun Earthquake) in the northern part of Hanaore Fault caused a deep-seated catastrophic landslide, so called Machii-Kuzure, which dammed the Ado River until its outburst at few weeks later. The most recent rainfall-triggered deep-seated catastrophic landslides occurred in 18-20 Aug 1992 by rainfall of ~600 mm/2 days; the event caused landslides with a volume of ~10^5 m^3 at two locations. The Hira Range is suitable to test knowledge obtained from Kii Mts as typical catastrophic landslide-prone area of accretionary sedimentary rock mountains.

3. METHODS

We employed GIS to identify landslide scars or deformations, and to analyze relationships among rainfall, topography, and landslide locations. A 10-m meshed DEM (Digital Elevation Model) distributed by GSI (Geospatial Information Authority), Japan was used for regional-scale topographic analyses. For a local scale, we used 1-m meshed DEMs obtained by Airborne LiDAR (Light Detection And Ranging) to delineate landslide scars or topographic signals of hillslope deformation.

First, we analyzed distributions of rainfall, topography and deep-seated landslides in a regional scale for the Kii Mts to establish their correlative regime to shape landscapes. A radar-based rainfall observation data as well as records of AMeDAS (Automated Meteorological Data Acquisition System) from JMA (Japan Meteorological Agency) were used for analyzing spatial pattern of orographic rainfall. Relationships between topographic relief or mean slope in a regional scale and rainfall spatial patterns are then compared by a cell-based correlative analysis on GIS. This approach provides a rough sketch of geomorphologic hazard assessment in the Kii Mts.

Then we focus into local scale to discuss linkage between long-term mechanical slope destabilization and slope-undercutting by river incision. Signals of gravitational hillslope deformation and profiles of slid hillslopes were analyzed using LiDAR-DEM at sites indicated by red-squares in **Fig. 1**. In this analysis the knowledge from Kii Mts was tested in the Hira range, where detailed spatial information of dense landslide scars and hillslope deformations are available by a LiDAR-DEM.

4. RESULTS AND DISCUSSION

4.1 Orographic rainfall, deep-seated landslides, and topography

The spatial pattern of rainfall at the 30Aug -Sep 5

2011 event exhibits a clear enhancement by orographic forcing, maximized its amount at south-east part of the Peninsula [**Fig. 2A**]. This pattern is typical for storms in this region, since another rainfall event at Jul 2011 shows an almost identical profiles across the peninsula, but only different in their magnitude [**Fig. 2B**].

The distribution of landslides are however not matched with the distribution of rainfall amount. The landslides occurred north-to-west outer rim of the rainfall center [**Fig. 2**]. This landslide distribution resembles these in the 1889 event that seems to have been caused by a similar rainfall condition[*Hirano*, 1984]. This evidently suggests the existence of landslide-prone zones in the central Kii Mts adjacent to the areas that receive highest rainfall amount enhanced by orographic effect.

Instead of the rainfall amount, rainfall anomaly explains well the landslide locations (**Fig. 3**). We defined the rainfall anomaly index as total rainfall amount during a given event normalized by local maximum-class daily rainfall. Here maximum-class daily rainfall were determined by 30-yrs AMeDAS records. The average of the five largest daily rainfall were calculated for each AMeDAS station, and then they were interpolated to estimate maximum-class daily rainfall in the inter-station areas. The list of ranked daily maximum rainfall is suitable for evaluating regional distribution of potential maximum-magnitude of rainfall events, because it is available most easily from JMA, and statistically reliable because of its number of records.

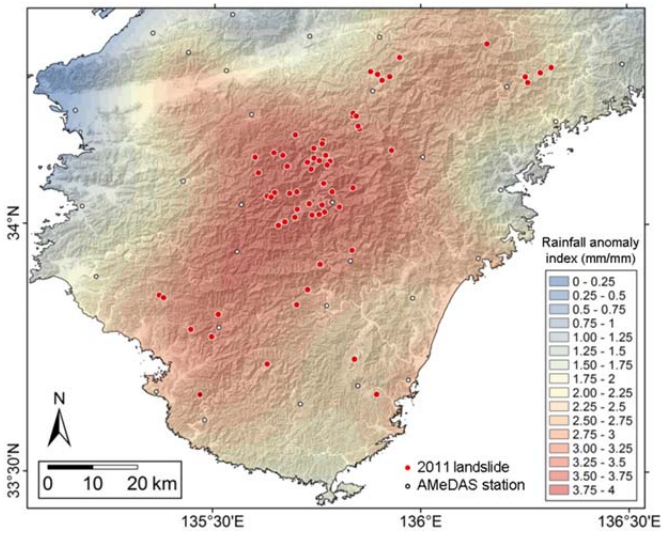

Fig. 3 Distribution of rainfall anomaly index for the 2011 landslide-triggering rainfall event. Rainfall anomaly index is defined as total rainfall amount during a given event normalized by local maximum-class daily rainfall estimated from 30-yr AMeDAS record.

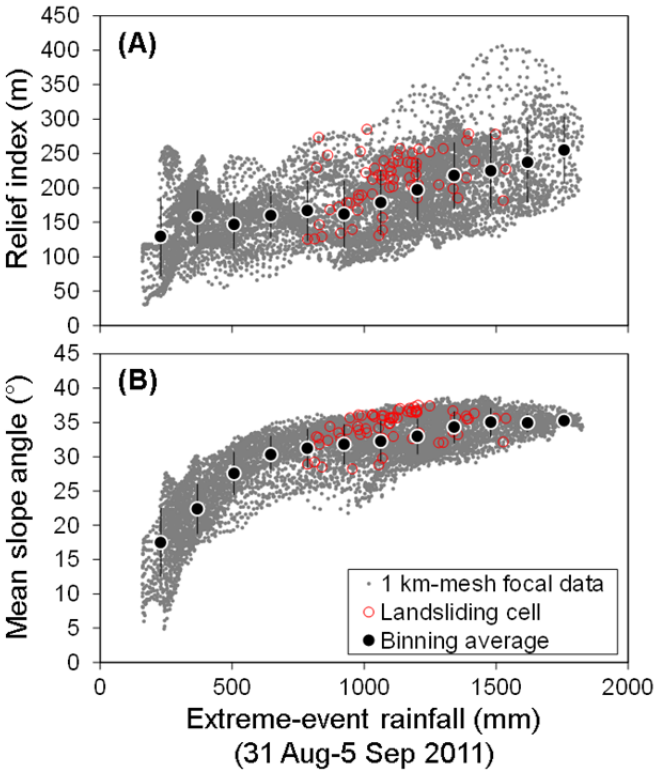

Fig. 4 Relationships between extreme-class orographic rainfall and topographic relief index (A), and mean slope (B) in the Kii Mts. The relief index was calculated for every 1 × 1 km cells on GIS, as standard deviation of altitude within a window of 100 km^2 circle (5.64 km radius). The mean slope was also calculated as cell-based average of hillslope angle in the same circle. Red open circles indicate cells of landsliding at the 2011 storm event.

Fig. 3 shows the spatial pattern of rainfall anomaly index for the 2011 event, which is concordant to the deep-seated landslide distribution. This fact indicates importance of relative rareness of rainfall magnitude, than absolute amount, for triggering deep-seated landslides. Landslide risk becomes rather higher when abnormal rainfall were supplied onto areas of normally less-rainfall. Similar trend has been found in analysis using Soil Water Index from JMA for the same event in the Kii Mts [*Saito et al.*, 2012].

Previously, it is known that rainfall threshold for shallow landsliding is smaller in less-rainfall area than rainy region [e.g., *Omura*, 1980; *Hayashi*, 1985]. However, for deep-seated bedrock landsliding, the 2011 event in Kii Mts is the initial case that the dependence of landslide susceptibility on rainfall rareness emerged clearly in a regional scale [**Fig. 3**]. This new finding reported here shed light on an unnoticed way for understanding and predicting locations of bedrock landslides.

Why does such regulation in landslide triggering appear in the extreme-class rainfall event? Since

every hillslopes present are a snapshot on a way of topographic evolution, landslide susceptibility is possibly affected by developmental stage of the landscape. We hypothesize that hillslopes become insensitive to rainfall to cause deep-seated landslides after they had experienced a number of extreme-class rainfall events enough to remove all weathered bedrock layers capable to be slid. In such stage, the landscape must be characterized by a threshold slope reflecting bedrock mass strength, and hillslopes should apparently become insusceptible to landsliding unless tectonic relief growth prepares potential slope instability. We need further evidence fully to test this hypothesis, but here we attempt to present data supporting the existence of a negative feedback between rainfall, landslides and topography.

To test this hypothesis, relationships between rainfall and topography (topographic relief and mean hillslope angle) were examined by GIS-based 10-m mesh DEM analyses. Topographic relief was calculated for every 1-km meshed cell as relief index, which is defined as standard deviation of altitude within a 100 km^2 circle (5.64 km radius) around the cell of interest. The mean value of cell-based hillslope angle were measured also for the same circle. The 1-km moving values of the relief index and the mean hillslope angle for this 100 km^2-circle window are compared to the 1-km meshed radar-based rainfall recorded at the 2011 landslide event as a typical extreme-class orographic rainfall.

Fig. 4 shows the relief index and mean slope plotted against amount of the extreme-class rainfall.

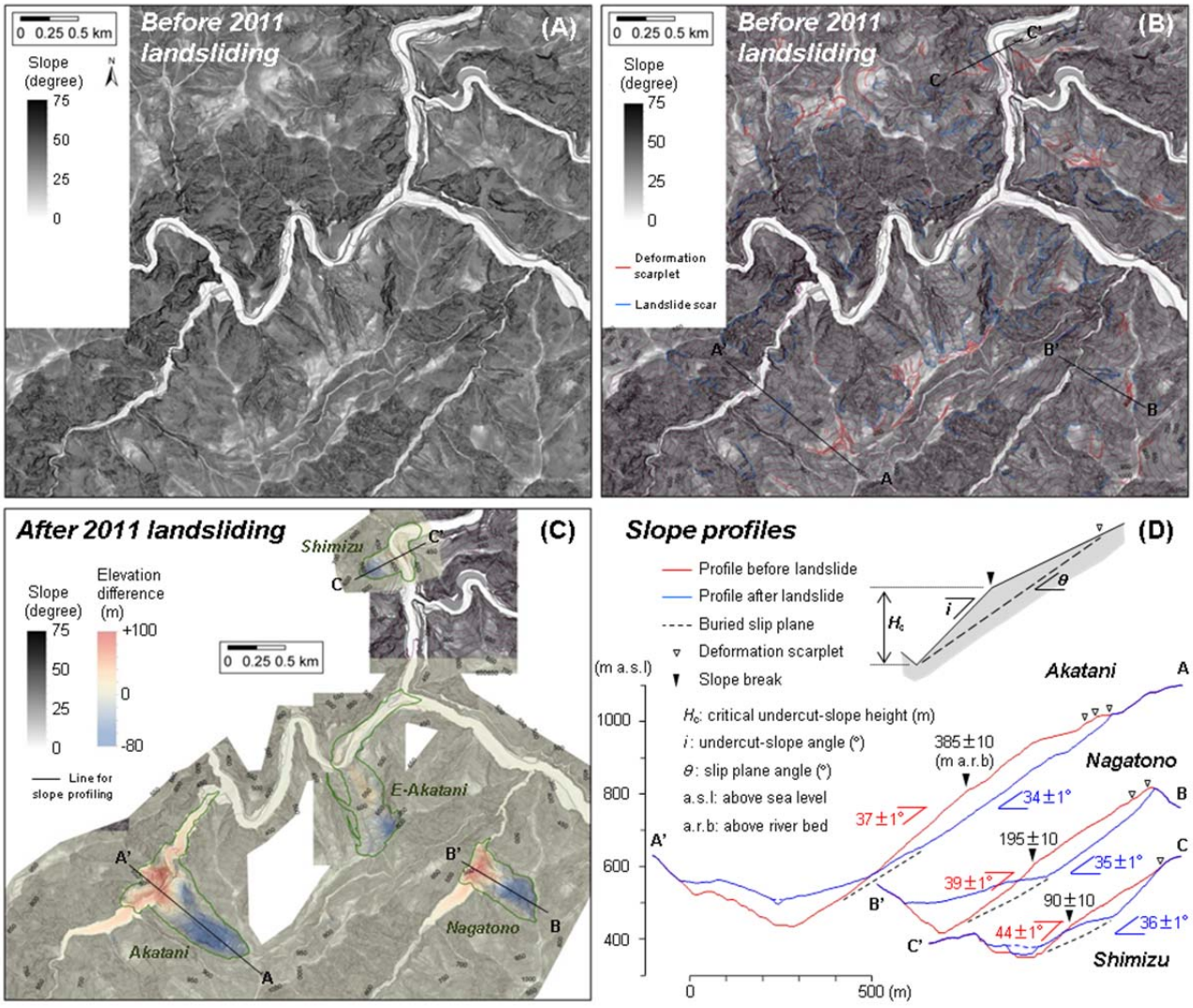

Fig. 5 Slope shade maps and slope profiles in the mid Totsukawa area, Kii Mts. (A) Plain slope shade map before the 2011 landslide event. (B) Slope shade map with delineation of landslide scars and deformation signals on the same area of (A). (C) Slope shade map after the 2011 landslide event with the elevation change by the landsliding. (D) Hillslope profiles before and after the landsliding. Height of slope brake and angles of undercut slope and slip plane are indicated. Schematic shows the definition of parameters for 2D wedge failure modeling by Eq. (1).

The relief index increases linearly with increasing rainfall, reflecting tectonic uplifting and river incision accompanied with bedrock landslides caused by orographic rainfall supply. The mean hillslope angle also increases with rainfall but seem to be saturated to form hillslope around 35 degrees. This threshold hillslope has deemed to be formed by bedrock landsliding [*Burbank et al.*, 1996; *Montgomery and Brandon*, 2002].

The topographic condition at locations of

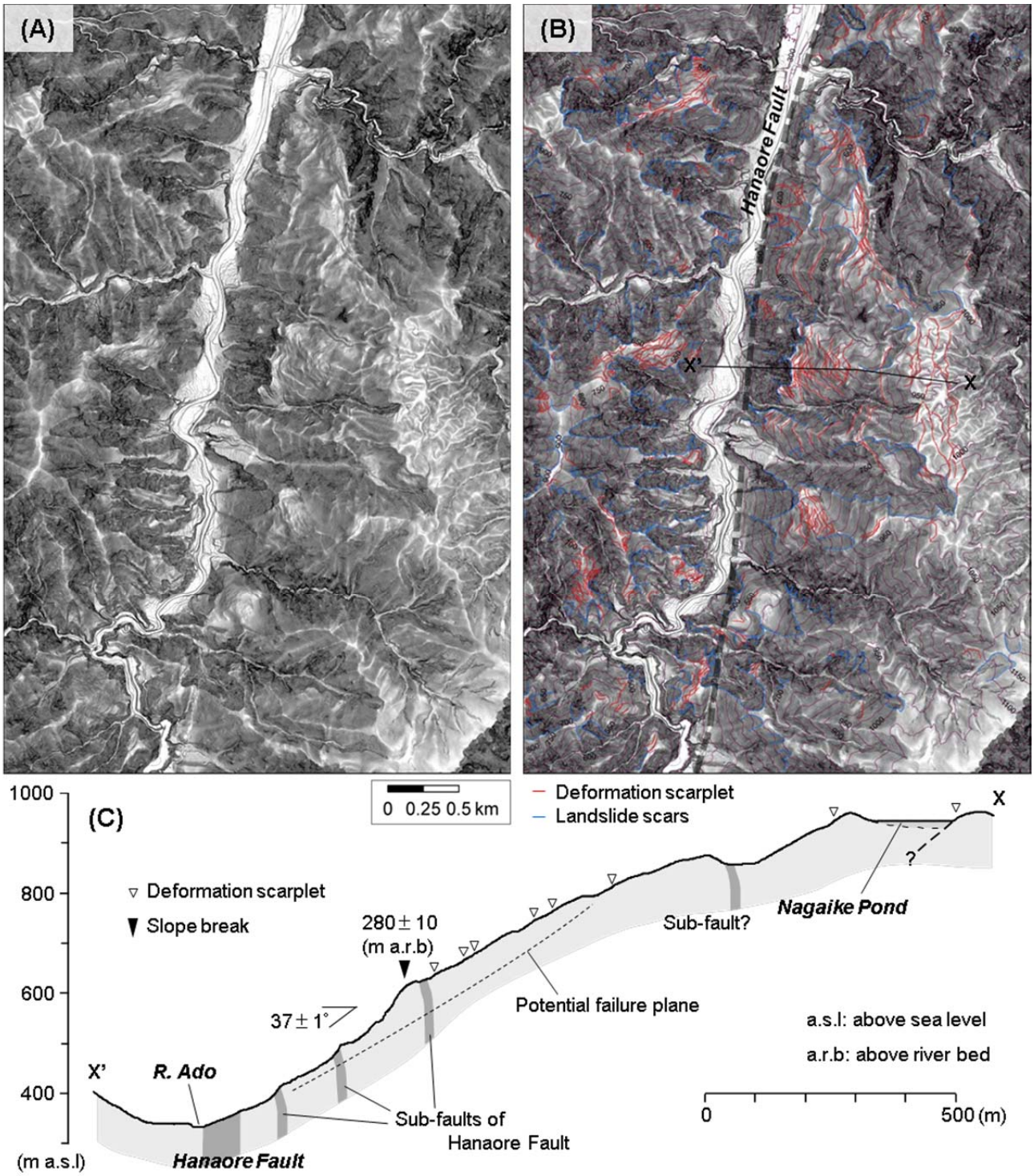

Fig. 6 Slope shade maps and slope profile in the western Hira Range. (A) Plain slope shade map. (B) Slope shade map with delineation of landslide scars and deformation signals on the same area of (A). (C) Typical hillslope profile of the dip slope at right-side valley slope of Ado River, along Haraore Fault. Height of slope brake and angle of undercut slope are indicated. A pond (Nagaike) has been formed on the low relief mountain top by subsidence of ridge crest, probably by gravitational whole slope deformation.

deep-seated catastrophic landslides in the 2011 event was not the highest in relief nor steepest in hillslope angle. The landslides occurred at cells with moderate relief index, 100-250 m, and mean slope over 30 degrees (cf. regional maximum relief index and slope are ~400 m and 35 degrees in the Kii Mts). This finding indicates that deep-seated landslides occur most frequently in the landscape in a pre-mature stage before establishment of possible highest-relief with steepest hillslope. For Kii Mts, the hazardous zone of deep-seated landslide is hence in areas with moderate relief as presented in **Fig. 1**, which is located out around the area of most enhanced orographic rainfall [**Fig. 2A**].

4.2 River incision and deep-seated landslides and deformations

The next question emerges on the point why landslides tend to occur most frequently in a pre-mature landscape. To answer this question we focus on hillslope profiles at landslide sites.

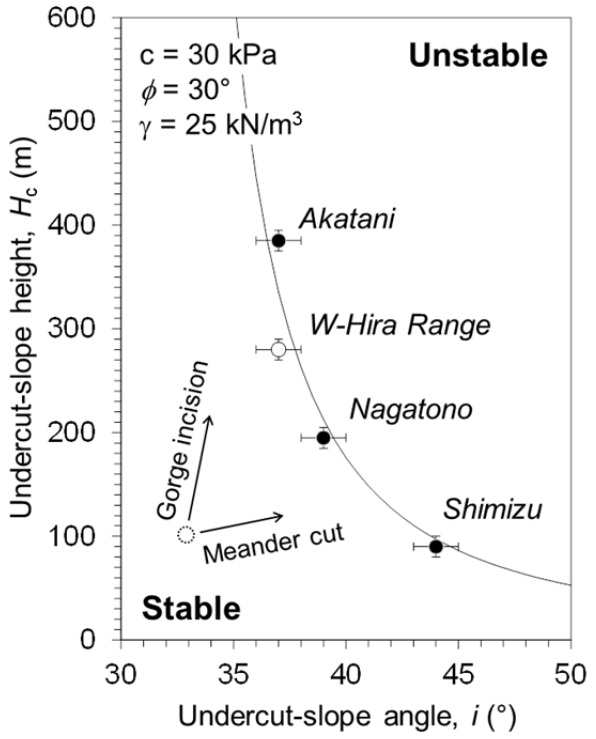

Fig. 7 Relationship between slope angle of undercut-part and height of slope break above river bed (cf. schematic in **Fig. 5D**), for landslides in the mid Totsukawa and deformed hillslope in the western Hira Range. Curve indicate boundary between stable and unstable conditions by Culmann's 2D wedge failure analysis for rock mass strength parameters of c = 30 kPa, ϕ = 30°, and rock mass unit weight γ = 25 kN/m^3. Undercutting by vertical gorge incision or lateral meander cutting would cause the hillslope destabilization as indicated as dotted open circle moving toward right-up reaching to the critical curve.

Fig. 5 shows slope-shade map and long-sectional profiles of hillslopes before and after the landslides in mid Totsukawa River where landslides concentrated in a narrow area. Many of landslides occur on north-face hillslopes; the slope direction is sub-parallel to the dip of beddings. Incision of Totsukawa River form an inner gorge, cutting the toe of hillslopes [**Figs. 5A, B, D**]. The steepened lower part of hillslopes generally leads to induce slope-clearing bedrock landslides as demonstrated by *Densmore et al.*, [1997]. Indeed these hillslopes slid along a slip plane connecting to the valley bottom [**Fig. 5D**]. Gravitational hillslope deformation is also observed in dip slopes in such incised valleys as a precursor of catastrophic landslides [**Figs. 5B, C**; *Hiraishi and Chigira*, 2011; *Chigira et al.*, 2013]. For areas outside from **Fig. 5**, majority of landslide scars in the Totsukawa River basin are located across the edge of dissection front [*Chigira*, 2013]. The formation of inner gorge (undercutting of hillslopes) thus seems to play an key role in a long timescale for the enhancement in susceptibility of deep-seated landslides in the pre-mature, being dissected landscapes.

The insight for controlling factors of deep-seated landslides from Kii Mts can be confirmed in another mountainous terrains underlain by accretionary sedimentary rocks: the western part of Hira Range [**Fig. 1**]. This area has a relief index of ~200 m with ~30 degrees of mean slope, characterized by a major, deeply-incised fault-along valley with right bank slopes dipping concordant with bedding. If the occurrence of deep-seated landslides is susceptible to topographic condition, we may observe many deep-seated landslide scars and hillslope deformations throughout this area.

The LiDAR-based mapping of landslide scars and deformation scarplets demonstrated, as expected, the instability of hillslopes in the western part of Hira Range. **Fig. 6** shows a slope shade map and hillslope profiles. Many landslide scars, various scarplets and large-scale deformations are evident on the hillslopes. The lower part of hillslopes has clearly been steepened by the incision of the Ado River along the Hanaore Fault. The spatial scales of landslides and hillslope deformations are similar to that in Kii Mts.

The scaplets appear on hillslopes in the Hira Range concentrated at elevations of 750-800 m, ~300 m above adjacent river bed. In the profile analysis, the deformed hillslopes in the western Hira Range [**Fig. 6C**] show striking similarity to the hillslopes in the Kii Mts, slid at the 2011 rainfall event [**Fig. 5D**]. They exhibit a comparable set of slope break and scarplets, and angle of potential slip

plane. This similarity may attribute to a common mechanism of slope instability, probably owing to undercutting by river incision.

This finding is not very surprising as the undercutting by rivers is one of the major trigger of large landslides in tectonically active mountain basins [e.g., *Tsou et al.,* 2014]. Of note is the scale accordance in hillslope relief and locations of scars or scarplets, in the two distinct regions both underlain by accretionary sedimentary rocks. This fact may reflect control on landsliding by height of undercut slope and rock mass strength as reported by *Schmidt and Montgomery* [1995]

The slope destabilization due to undercutting can be modeled most simply by Culmann's 2D wedge failure analysis [*Matsukura*, 1987; *Schmidt and Montgomery*, 1995], in which critical height of steepened lower part of the undercut slope is formulated as

$$H_c = \frac{4c}{\gamma} \frac{\sin i \cos \phi}{1 - \cos(i - \phi)} \qquad (1)$$

where H_c is critical height of hillslope undercut (i.e., height of slope break above river bed) [m], i is angle of hillslope undercut [°] [cf. **Fig. 5D**], c is rock mass cohesion [kPa], ϕ is angle of shearing resistance [°], γ is rock mass unit weight [kN/m^3]. In this formulation, the angle of failure plane θ [°] [cf. **Fig. 5D**] is given as

$$\theta = \frac{\phi + i}{2} \qquad (2)$$

as shearing resistance along the slip plane should be maximized at the critical state. Substituting the actual angles of i and θ from the mid Totsukawa landslides [**Fig. 5D**] to Eq. (2), we can estimate ϕ to as ~30° for dip slope of accretionary sedimentary bedrock.

The relationship between H_c and i is plotted for the actual slid hillslopes for the case of the mid Totsukawa landslides (solid circles in **Fig. 7**). H_c decreases with increasing i as is modeled by Eq. (1), that is fit by parameters of c = 30 kPa, ϕ = 30°, and γ = 25 kN/m^3 (solid curve in **Fig. 7**). The values of H_c and i from the western Hira Range is also on the model curve (open circle in **Fig. 7**). This accordance between model and actual slid/deformed hillslope indicates that undercutting by river incision is the major control in destabilization of hillslopes. The best-fit values of c and ϕ are comparable to strength of highly weathered rock mass (D-class), even though the actual slip planes are located at depths of dozens of meters below surface [**Figs. 5C, D**]. This implies that discontinuity sub-parallel to slope in bedrock with only weak asperity is crucial for initiation of deep-seated landsliding in accretionary complex.

In the **Fig. 7**, given a stable hillslope (e.g., H = 100 m and i = 33°: open dotted circle), it would become unstable by moving toward right-up side in the diagram. Possible geomorphic processes for this destabilization are downward incision of gorge and/or lateral meander cutting. The degree of undercutting can easily be calculated by hillslope long-sectional profiling on GIS. Thus we may be able to evaluate landslide hazard by such topographic analysis with the modeled critical instability curve, which allows us to plot every single undercut hillslope on the slope-stability phase diagram.

In the Kii Mts, however, tectonic effect as well as rock-type control could potentially superimpose the correlations between rainfall and topographic proxies [**Fig. 4**]. Such risk of potential bias has not been checked up in the present paper. As a next task, evaluation is required from geologic and tectonic standpoints, such as density analysis of paleo landslides in each geologic band, and reconstruction of 'erosion-wave' propagation through the mountainous basin by measuring spatial distribution of incision rates of rivers.

Unlike the Kii Mts, active sub-faults accompanying with the Hanaore Fault may affect the slope destabilization in the western Hira Range. Along fault, N-S oriented lineaments were observed clearly on the map in the Hira Range [**Fig. 6B**], while this kind of systematic lineaments are unclear in the Kii Mts [**Fig. 5**]. Evaluation for role of this type of geologic discontinuity in slope destabilization as well as subsoil hydrological processes is also left for future work. Understanding of subsurface hydrological process including behavior of deep bedrock groundwater is necessary for evaluating effect of preceding rainfall and predicting timing of deep-seated catastrophic landslides.

5. CONCLUSIONS

The spatial pattern of orographic rainfall is closely related to the topographic relief and mean hillslope angle, and hence occurrence of deep-seated catastrophic landslides in the Kii Mts, reflecting the stages of landscape evolution. The spatial distribution of 2011 landslides is concordant with rainfall anomaly rather than absolute rainfall amount. The landslide-prone area is located out around the most enhanced orographic rainfall

center, with relief index (altitude dispersion in a 100 km^2 circle window) of 100-250 m and mean slope over 30°. These areas are not the most highest-relief nor steepest zones in the Kii Mts, but exhibit a pre-mature landscape characterized by hillslope undercutting by river incision. Similar inner-gorged landscape is also evident in the western Hira Range, along a major active-fault incised-valley. A simple wedge failure modeling for such undercut hillslope well explains the instability of actual slid/deformed hillslopes, indicating the significance of downward incision of gorge or lateral meander cutting for long-term hillslope destabilization.

ACKNOWLEDGMENT: Data of LiDAR-DEM in the Kii Mts were provided by Ministry of Land, Infrastructure, Transport and Tourism of Japan, and the Nara Prefectural Government. This research is supported by KAKENHI (23654172, 24300321), and CREST, JST.

REFERENCES

Burbank, D.W., Leland, J., Fielding, E., Anderson, R. S., Brozovic, N., Reid, M. R. and Duncan, C. (1996): Bedrock incision, rock uplift and threshold hillslopes in the northwestern Himalayas, Nature, Vol. 379, pp. 505-510.

Burbank, D.W., Blythe, A.E., Putkonen. J., Pratt-Sitaula, B., Gabet, E., Oskin, M., Barros, A., and Ojha, T.P. (2003): Decoupling of erosion and precipitation in the Himalayas, Nature, Vol. 426, pp. 652-655.

Chigira, M. (1992): Long-term gravitational deformation of rocks by mass rock creep, Eng. Geol., Vol. 32, pp. 157-184.

Chigira, M. (2000): Geological structures of large landslides in Japan. J. Nepal Geol. Soc., Vol. 22, pp. 497-504.

Chigira, M. (2009): September 2005 rain-induced catastrophic rockslides on slopes affected by deep-seated gravitational deformations, Kyushu, southern Japan, Eng. Geol., Vol. 108, pp. 1-15.

Chigira, M. (2013): Deep-seated catastrophic landslides ― where are potential sites? Kinmiraisha, Nagoya, 231p (in Japanese).

Chigira, M., Tsou, C.-Y., Matsushi, Y., Hiraishi, N. and Matsuzawa, M. (2013a): Topographic precursors and geological structures of deep-seated catastrophic landslides caused by Typhoon Talas, Geomorph., Vol. 201, pp. 479-493.

Chigira, M., Hariyama, T. and Yamasaki, S. (2013b): Development of deep-seated gravitational slope deformation on a shale dip-slope: observations from high-quality drill cores, Tectonophysics, Vol. 605, pp. 104-113.

Densmore, A.L., Anderson, R.S., McAdoo, B.G. and Ellis, M.A. (1997): Hillslope Evolution by Bedrock Landslides, Science, Vol. 275, pp. 369-372.

Gabet, E.J., Pratt-Sitaula, B.A. and Burbank, D.W. (2004): Climatic controls on hillslope angle and relief in the Himalayas, Geology, Vol. 32, pp. 629-632.

Hayashi, S. (1985): Some relationships between the landslide-area ratio and hydrologic data, J. Jap. For. Soc., Vol. 67, pp. 209-217 (in Japanese with English abstract).

Hirano, M., Suwa, H., Ishii, T., Hujita, T. and Gocho, Y. (1984): Reexamination of the Totsukawa hazard in August 1889 with special reference to geologic control of lange scale landslides, Reexamination of the Totsukawa Hazard in August 1889 with Special Reference to Geologic Control of Lange Scale Landslides, Annuals. Disaster Prevention Res. Inst., Kyoto Univ., Vol. 27B-1, pp. 369-386 (in Japanese with English abstract).

Hiraishi, N. and Chigira, M. (2011): Formation of inner gorge and occurrence of gravitational slope deformation in the central Kii Mountains, Trans. Japan. Geomorph. Union, Vol. 32, pp. 389-409 (in Japanese with English abstract).

Matsukura, Y. (1987): Evolution of valley side slopes in the "Shirasu" ignimbrite plateau. Trans. Japan. Geomorph. Union, Vol. 8, pp.41-49.

Mizuyama, T., Mori, T., Sakaguchi, T. and Inoue, K. (2011): Landslide dams and countermeasure method in Japan, Kokon Shoin, Tokyo, 205p (in Japanese).

Montgomery, D.R. and Brandon, M.T. (2002): Topographic controls on erosion rates in tectonically active mountain ranges, Earth Planet. Sci. Lett., Vol. 201, pp. 481-489.

Omura, H. (1980): Fundamental study on forecasting of landslide area (I) ―Relation between total precipitation, resistance index and landslide area ratio, Shin-Sabo (J. Erosion-Contr. Eng. Soc.), Vol. 117, No. 2, pp. 15-25.

Schmidt, K.M. and Montgomery, D.R. (1995): Limits to relief, Science, Vol. 270, pp. 617-620.

Saito, H. and Matsuyama, H. (2012): Catastrophic landslide disasters triggered by record-breaking rainfall in Japan: their accurate detection with normalized Soil Water Index in the Kii Peninsula for the year 2011, SOLA, Vol. 8, pp. 81-84.

Sasahara, K. Sakurai, W., Kato, H., Shimada, T. and Ono, N. (2012): Geomorphologic characteristics of slopes where landslides occurred by LiDAR: case study of landslides occurred at eastern part of Kochi due to Typhoon No.6, 2011, Proc. DPRI Topical Research Meeting 23C-03, pp. 1-10 (in Japanese with English abstract).

Tabata S., Mizuyama T. and Inoue K. (2002): Landslide dams and Disaster, Kokon Shoin, Tokyo, 205p (in Japanese).

Tsou, C.-Y., Chigira, M., Matsushi, Y., Chen, S.-C., (2014): Fluvial incision history that controlled the distribution of landslides in the Central Range of Taiwan, Geomorph., Vol. 226, pp. 175-192.

Yamada, M., Matsushi, Y., Chigira, M. and Mori, J. (2012): Seismic recordings of landslides caused by Typhoon Talas (2011), Japan, Geophys. Res. Lett., Vol. 39, L13301.